JOURNAL OF MATERIALS SCIENCE 33 (1998) 2551–2562

Fracture behaviour of polypropylene/glass bead elastomer composites by using the essential work-of-fracture method[§]

D. E. MOUZAKIS*, F. STRICKER‡, R. MÜLHAUPT‡, J. KARGER-KOCSIS*‖
*Institut für Verbundwerkstoffe GmbH, Universität Kaiserslautern, Pf. 3049, D-67663 Kaiserslautern , Germany
‡Freiburger Materialforschungszentrum, Albert-Ludwigs-Universität, Stefan-Meier-Strasse 21, D-79104 Freiburg, Germany
E-mail: karger@ivw.uni-kl.de

The plane-stress static fracture response of blends composed of isotactic polypropylene glass beads (GBs) and an elastomer of styrene/ethylene–butylene/styrene type (SEBS) in both the ungrafted state and the grafted state with maleic acid anhydride (SEBS-g-MA) was studied at room temperature and $v = 1$ mm min^{-1} cross-head speed. The volume fraction of GBs was kept constant (10 vol%) whereas that of the elastomer was set for 5 and 20 vol%, respectively. Deeply double edge-notched specimens of different ligaments were cut from pressed sheets of about 1 mm thickness and subjected to tensile tests at ambient temperature. The development of the plastic and process zone was studied *in situ*, i.e., during loading of the specimens, by light microscopy and infrared thermography. From the specific work of fracture versus ligament length plots, the essential and non-essential work of fracture components were determined. It was established that the essential work-of-fracture approach works well for these hybrid composites. The specific essential work of fracture, w_e, increased with increasing amount of the rubbery modifier but depended on its type. Grafting changed the morphology of the composites (SEBS-g-MA covered the GBs, whereas SEBS was present as an additional dispersed phase) and affected both the essential (slightly) and the non-essential or plastic work (considerably) terms. It was established that SEBS-g-MA is a less efficient toughener than SEBS because of the substantial differences in the related failure modes. © *1998 Chapman & Hall*

1. Introduction

The essential work of fracture (EWF) approach [1, 2] is an attractive way of determining the fracture behaviour of ductile semicrystalline polymers and polymer matrix composites. The corresponding experiments using deeply double-edge-notched tensile (DDENT) specimens are relative simple to perform and offer the chance of using a variety of *in-situ* observation techniques, such as light microscopy (LM) and infrared thermography (IT). The EWF method has been nowadays widely adopted for the study of the fracture of ductile polymers [3–6].

Tough polypropylene (PP) has an attractive price and exhibits good mechanical properties and thermal resistance; its moderate fracture performance, especially at subambient temperatures, has always been an obstacle for both engineering and less demanding applications. The low-temperature impact resistance of PP is usually improved by melt blending (incorporation of various elastomers in PP [7]) or by copolymerization techniques (*in-situ* formation of a dispersed elastomer phase within the PP matrix [8]). However, this toughness upgrade is achieved at the cost of stiffness and strength characteristics. In order to improve the stiffness to toughness balance for elastomer-toughened PP, fillers (e.g., talc, calcium carbonate) or reinforcing fibres (e.g., short glass fibres) are added [9]. Glass beads (GBs) also prove to be an excellent choice for filling. Because of their regular spherical shape, the mechanical response of the filled PP is isotropic, making it a suitable system for modelling and theoretical studies (e.g., [10, 11]).

In this paper, effort has been undertaken to study the fracture behaviour of hybrid composites consisting of isotactic polypropylene (PP), thermoplastic styrenic elastomer and GBs by means of post-yield fracture mechanics and specifically utilizing the EWF theory. These hybrid systems [12] have already been examined with respect to their tensile stiffness, strength and high-speed impact fracture behaviour.

[§] Presented at the Conference on Interfacial Phenomena in Composite Materials 1–3 September 1997, Eger, Hungary.
‖ To whom all correspondence should be addressed.

2. Experimental procedure

2.1. Materials and specimen preparation

The polymers used in this study were all commercial grades supplied by Shell. The PP (KM 6100) serving as matrix for the hybrid composites showed the following characteristics: $M_n = 46500\ g\,mol^{-1}$; $M_w/M_n = 7.6$;, melt flow index, 3.5 g/10 min at 230 °C and 2.16 kg load. The elastomer was the thermoplastic polystyrene–block–poly(ethene-co-butene-1)– block–polystyrene (Kraton G1652), abbreviated hereafter as SEBS ($M_n = 90\,000\ g\,mol^{-1}$; polystyrene content of about 29 wt%). The corresponding maleinated version, SEBS-g-MA (Kraton FG1901X), was grafted with 2 wt% maleic anhydride. Surface-treated GBs (5000 CP-03 of Potters-Ballotini, Kirchheim-Bolanden, Germany) of about 5 μm average diameter were used as filler. The GBs were functionalized by 0.02 wt% of aminopropyl-trimethoxysilane in order to promote the adhesion to both the PP matrix and the elastomer. Furthermore, a thermal stabilizer consisting of Irganox 1010–Irgafos 168 (4:1 weight ratio, both of them from Ciba, Basel, Switzerland) was used in 0.2 wt% to prevent thermal decomposition during melt blending.

Circular plates of about 150 mm diameter and 2 mm thickness were compression moulded under identical conditions. Melt blending was performed in a kneader (Haake Rheomix 90, Karlsruhe, Germany), equipped with a 60 ml mixing chamber, pre-heated to 240 °C. First the PP was kneaded together with the stabilizers for 1.5 min prior to dosage with the GB filler. The melt kneading was followed at 60 rev min^{-1} for a further minute before the elastomer was introduced. After mixing for a further 4 min the sample was quickly removed from the kneader and pressed (Polystat 100 from Schwabenthan, Berlin, Germany) between metal films. In the press cycle the blend was kept at 250 °C for 10 min followed by quenching (water cooling of the press plates) to ambient temperature. For all blends the filler content was constant, i.e., 10 vol%, whereas the content of the elastomeric modifier was varied (0, 5 and 20 vol%). The systems investigated were the following: (a) pure PP (only stabilizer added); (b) PP with 10 vol% GBs; (c) PP with 10 vol% GBs and 5 vol% SEBS; (d) PP with 10 vol% GBs and 5 vol% SEBS-g-MA; (e) PP with 10 vol% GBs and 20 vol% SEBS; (f) PP with 10 vol% GBs and 20 vol% SEBS-g-MA.

The rectangular (length × width = 90 × 25 mm) DDENT specimens seen in Fig. 1, of varying ligaments (from 5 to 20 mm) were sawn from these plates. The upper ligament was larger than the threshold value (width/3) prescribed in the ESIS protocol [13] but it has been proven [4, 5, 14] that this upper threshold limit does not always represent the true situation. Deep blunt notches were induced on both sides of the specimens by a wheel saw. The sawn notches were sharpened by tapping with a fresh razor blade to produce the sharp pre-crack required.

2.2. Work-of-fracture method

Linear elastic fracture mechanics is often used to characterize the fracture behaviour of many polymeric materials [15]. The critical stress intensity factor and critical strain energy release rate proved to be material constants under certain testing conditions that ensure small scale yielding in the specimens. However, this approach cannot be adopted for toughened polymers which exhibit gross yielding during fracture. For the assessment of the fracture toughness of such ductile polymers, the EWF method is gaining acceptance. According to the EWF theory, the total energy required to fracture a pre-cracked specimen can be

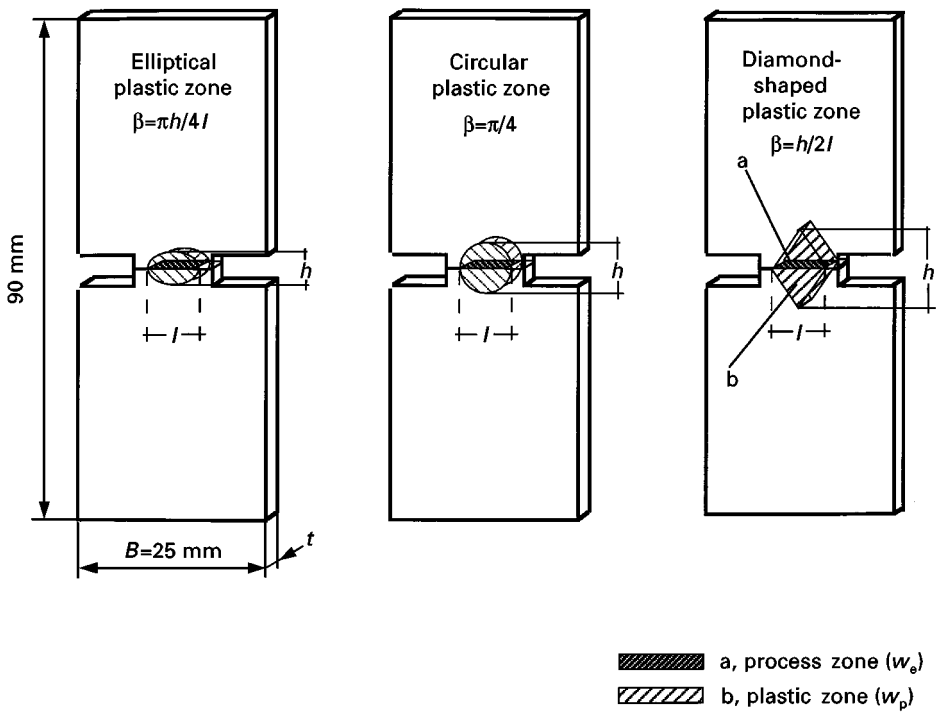

Figure 1 DDENT specimens used showing different types of the plastic zone along with the definition of the shape parameter, β.

distinguished by two components: the essential work of fracture, W_e, and the non-essential or plastic work of fracture, W_p. The first term relies on the energy which is needed to fracture the polymer in the process zone (net cross-section of the DDENT specimen; see Fig. 1) and thus generate new surfaces. W_p is the actual energy dissipated in the outer plastic region of the crack zone where various types of deformation may be at work. Therefore, W_e is only surface related, whereas W_p is a function of the deformed plastic zone volume. The total fracture energy, W_f, calculated from the surface of the force–displacement curves, can thus be expressed by

$$W_f = W_e + W_p \quad (1)$$

Considering the aforementioned surface dependence (lt) and volume dependence (l^2t) of the constituent terms, Equation 1 can be rewritten using the specific terms of essential and non-essential work of fracture:

$$W_f = w_e lt + \beta w_p l^2 t \quad (2)$$

$$w_f = \frac{W_f}{lt} = w_e + \beta w_p l \quad (3)$$

where l is the ligament length, t is the specimen thickness and β is a shape factor related to the form of the plastic zone. Obviously, w_e can be estimated from the interception of the linear regression of the plot of w_f versus l with the w_f axis. On the other hand, w_p can be calculated from the slope of the linear regression w_f versus l, provided that the shape of the plastic zone is well defined (cf. Fig. 1).

It was claimed by Karger-Kocsis [4] and Karger-Kocsis *et al.* [5], contrary to objections [16], that the specific essential work of fracture does represent a true material parameter when the EWF method is applied for suitable polymers.

Static tensile tests on DDENT specimens were performed on a Zwick 1248 (Ulm, Germany) machine at room temperature at a cross-head speed $v = 1\ \text{mm min}^{-1}$. The specimens were loaded to failure and force–time traces were plotted on line. W_f was calculated from the area beneath the related force–displacement (F–x) curves.

2.3. Development of the plastic zone and failure assessment

2.3.1. Light microscopy (LM)

A travelling optical stereomicroscope (Olympus, Hamburg, Germany) equipped with a 35 mm photocamera was employed to observe and record the fracture process DDENT specimens of all types of hybrid composite during static loading. A similar device was used to specify the final shape (as depicted in Fig. 1) and size of the plastic zone of the fractured specimens.

2.3.2. Infrared thermography (IT)

IT is a powerful technique to study the failure mode in polymers [4, 5, 15] ensured by their inherently low heat conductivity. IT provides information about the mode and actual magnitude of fracture in terms of thermal emission. A Hughes infrared camera (Portland, Oregon, USA) connected via RGB channels to a Sony digital monitor and VHS video recorder helped to monitor the fracture of the specimens *in situ*. Colour prints showing the actual temperature field in the process and plastic zones were made by means of a Mitsubishi video printer.

2.3.3. Scanning electron microscopy

The fracture surface (i.e. the process zone) of the specimens was studied in a scanning electron microscope (JEOL JSM 5400, Tokyo, Japan) after sputtering it with gold. Scanning electron microscopy (SEM) pictures were taken also from the surface plastic zone.

3. Results and discussion

3.1. Essential work of fracture

Typical engineering stress–strain (σ–ε) diagrams for all types of hybrid composite are shown in Fig. 2. For comparison purposes the same ligament ($l = 15$ mm) was selected. The plain PP experiences a fully brittle behaviour with no sign of plasticity (curve a). Because of the addition of GB, instead of brittle fracture, a pronounced plastic deformation appears. The elongation, ε_b, to failure increases up to about 15%, whereas the net section stress, σ_n, falls to about 25 MPa (see curve b). An even more ductile behaviour was observed for the composite containing 5 vol% SEBS (see curve c). A small increase in ε_b (up to 17%) and a very stable crack propagation characterize the related σ–ε curve. With increasing SEBS content (i.e., 20 vol%), σ_n decreased to about 22 MPa, while ε_b surpassed 20% (curve e in Fig. 2). Thus the increasing amount of SEBS improved the material ductility but impaired the strength, as expected. Curves d and f in Fig. 2 reflect the fracture of the hybrids containing 5 and 20 vol% SEBS-g-MA, respectively. Although the σ_n values of the composites containing elastomer are similar, those with the maleinated version exhibit clearly reduced ductility. The rationale behind this "stiffening" mechanism will be discussed later in connection with the fractographic results. It is noteworthy that the maximum net section stress of the hybrid composites (see σ_n data in Fig. 2) were below the threshold $1.15\sigma_y$ (criterion used for validation of the EWF tests on DDENT specimens [13]) where σ_y is the yield strength determined on dumbbell specimens.

The specific total work of fracture, w_f, for each specimen (as calculated from the F–x diagrams and related to the ligament area) versus ligament, l, curves are presented in Fig. 3. The w_e values can be read from the interception with the y axis of the linear regression lines w_f versus l. The w_e values together with the related correlation coefficients are listed in Table I. Incorporation of the thermoplastic elastomer (especially the SEBS) in the base composite (i.e., PP + 10 vol% GBs) seem to enhance fracture toughness. The effects of elastomer maleination are clearly displayed in both Fig. 3 and Table I. The SEBS-g-MA containing blends show an impaired toughness

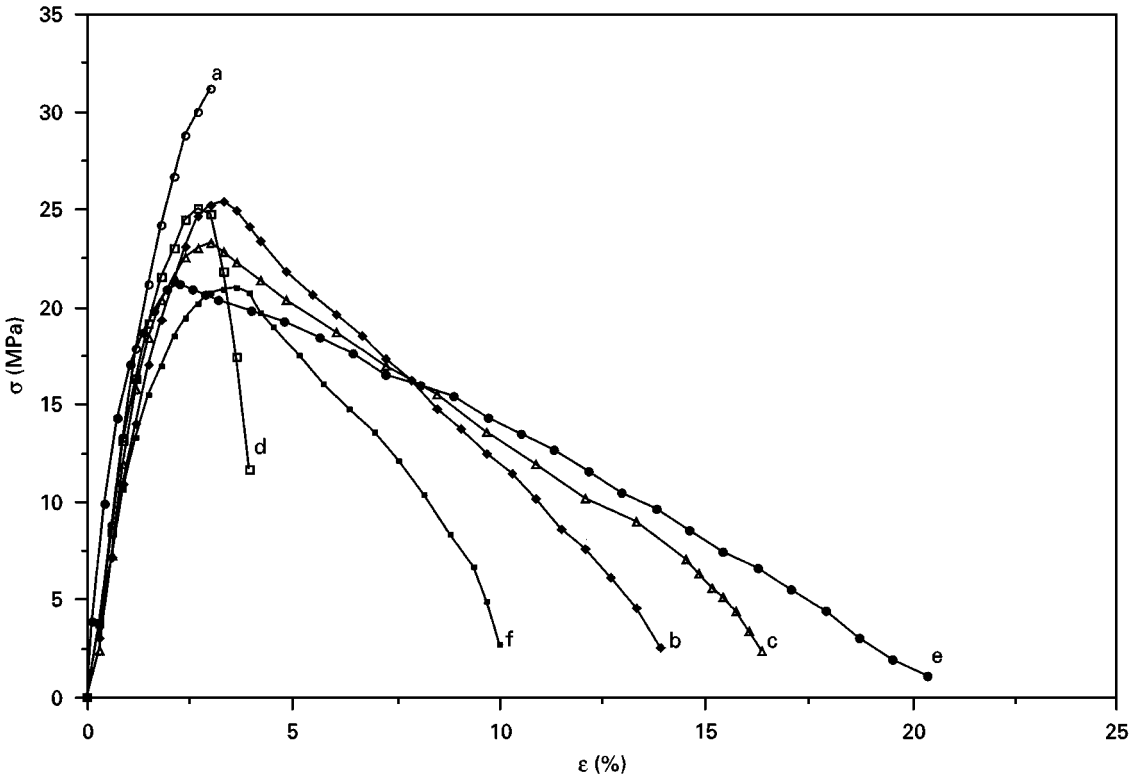

Figure 2 Stress-strain (σ–ε) curves of DDENT specimens at the same ligament length (l = 15 mm) for the hybrid composites studied. (○), curve a, PP; (◆), curve b, PP + 10 vol% GBs; (△), curve c, PP + 10 vol% GBs + 5 vol% SEBS; (□) curve d, PP + 10 vol% GBs + 5 vol% SEBS-g-MA; (●), curve e, PP + 10 vol% GBs + 20 vol% SEBS; (■), curve f, PP + 10 vol% GBs + 20 vol% SEBS-g-MA.

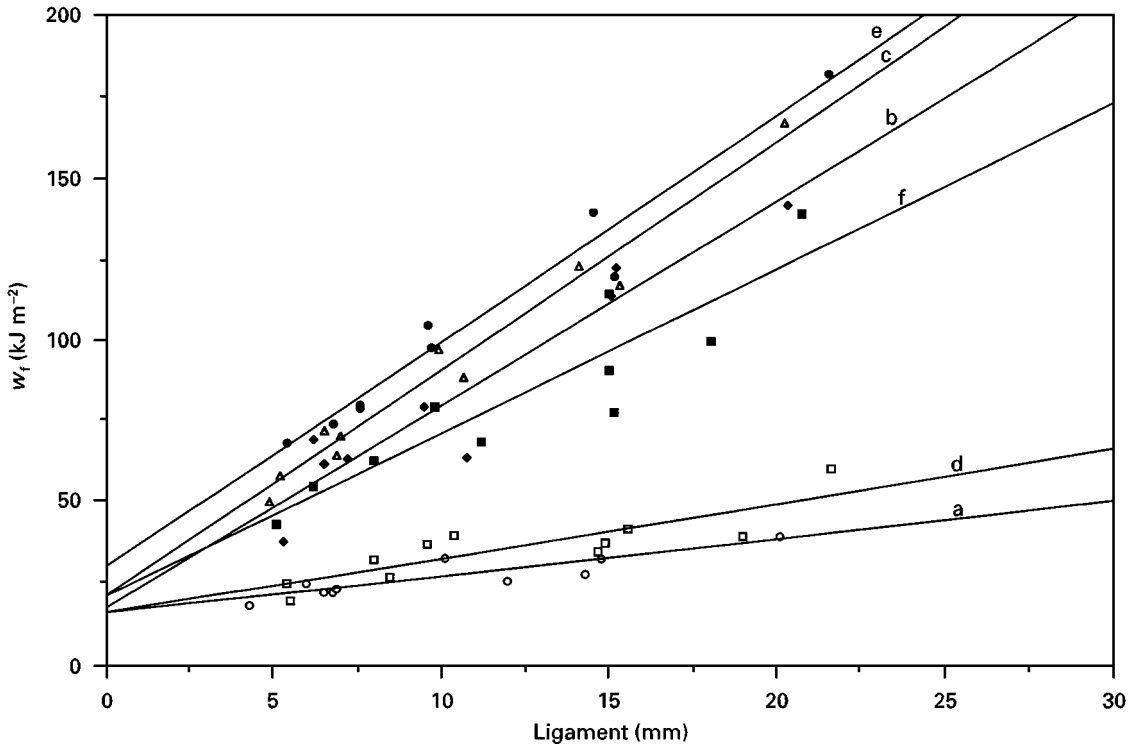

Figure 3 Total specific energy to fracture, w_f, plotted against the ligament size, l, for all systems. For designations see Fig. 2.

compared with the composites containing SEBS. The w_e values of the PP and base composite are almost identical, as expected. However, w_e increases with increasing elastomer amount. This increase is, however, strongly dependent on the type of the elastomer (SEBS-g-MA is less effective than the SEBS version). A large difference was found with respect to the slope (i.e., βw_p term) of the w_f versus l curves (cf. Fig. 3 and Table I), to which attention will be paid next.

TABLE I Essential work of fracture, w_e, and non-essential work of fracture, w_p, data together with the shape parameters, β, derived from LM, for the hybrid composites studied

Hybrid composite	w_e (kJ m^{-2})	βw_p (MJ m^{-3})	R^2	β	w_p (MJ m^{-3})
PP	≈ 15	1.17	0.809	—[a]	—[a]
PP + 10 vol% GBs	≈ 16	6.36	0.905	0.249	25.5
PP + 10 vol% GBs + 5 vol% SEBS	≈ 20	7.07	0.972	0.257	27.5
PP + 10 vol% GBs + 5 vol% SEBS-g-M	≈ 15	1.73	0.751	0.037	46.7
PP + 10 vol% GBs + 20 vol% SEBS	≈ 29	7.02	0.962	0.329	21.3
PP + 10 vol% GBs + 20 vol% SEBS-g-M	≈ 20	5.11	0.834	0.165	31.0

[a] Cannot be determined.

3.2. Non-essential work of fracture

In order to calculate the specific non-essential work of fracture, w_p, first the shape parameter, β, of the plastic zone should be determined. Therefore, the plastic zone heights, h (see Fig. 1), were plotted as a function of the corresponding ligaments, and linear regression lines were fitted to them (Fig. 4). According to Equation 3, the slope of the w_f versus l curves is βw_p. β, on the other hand, can be determined by considering the h versus l slope, provided that the shape of the plastic zone is well defined (see Fig. 1). Accepting an elliptical plastic zone, as confirmed by LM (see Figs 6 and 7), β equals $\pi h/4l$ [13]. A simple method to confirm the elliptical shape of the plastic zone is to plot the calculated plastic area values (accepting an ellipse for the shape of the plastic zone: see above) against the ligament size. In Fig. 5 the curves fitted to the experimental points confirm the statement about the elliptical shape of the plastic zone. Furthermore, the reduction in the plastic zone in composites containing SEBS-g-MA becomes obvious. This implies restricted plastic deformation.

The terms related to the plastic work (i.e., βw_p, β and w_p) are also given in Table I. Table I clearly demonstrates that incorporation of GBs triggers a considerable plastic deformation. A further increase in both slope, βw_p, and shape parameter, β, can be achieved by adding SEBS, whereas the incorporation of SEBS-g-MA yields the opposite tendency. With knowledge of the β parameters, w_p can also be quantified (see Table I). Compared with the related value of the base composite, w_p seems to pass through a maximum as a function of the elastomer amount. The related function is obviously dependent on both amount and type (i.e., grafted or not) of the elastomer. The finding that the w_p data for the hybrids with SEBS-g-MA are superior to those with SEBS should have some microstructural explanation. It is reasonable to suppose in the first approximation that the adhesion between the components of the hybrid with SEBS-g-MA is better. Furthermore, the decrease in w_p

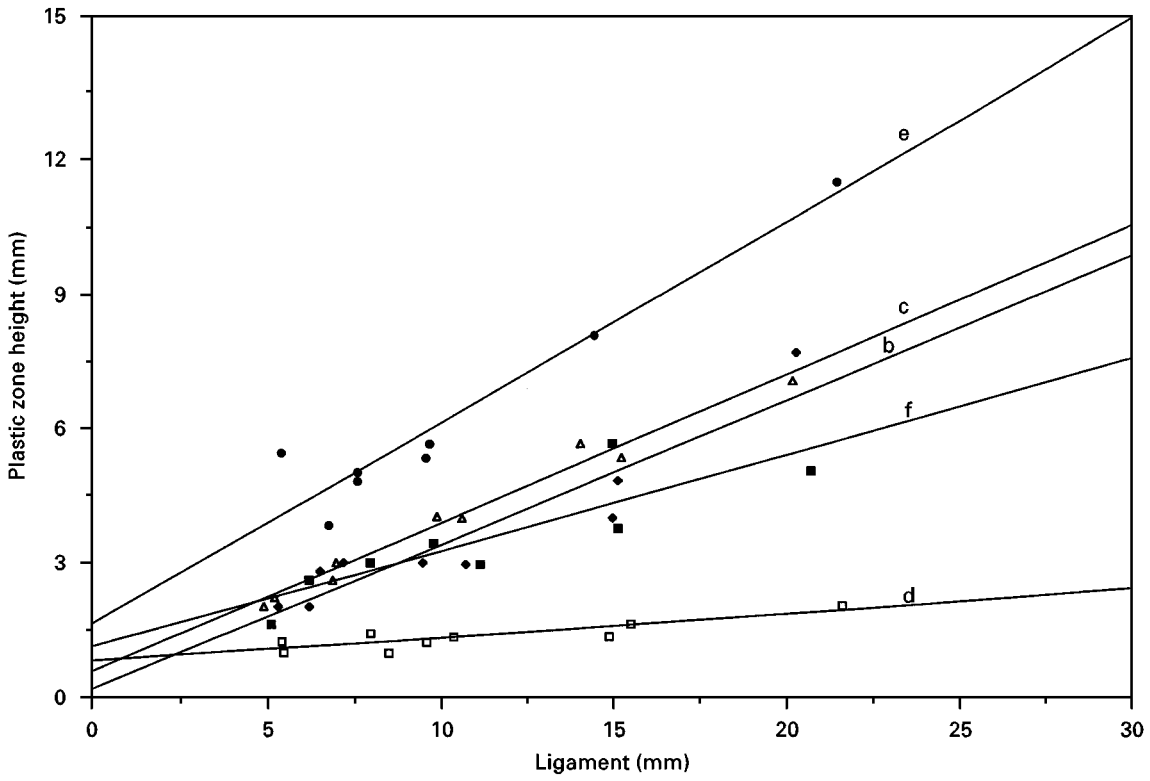

Figure 4 The height, h, of the plastic zone as a function of the ligament length, l, for all hybrid composites. For designations see Fig. 2.

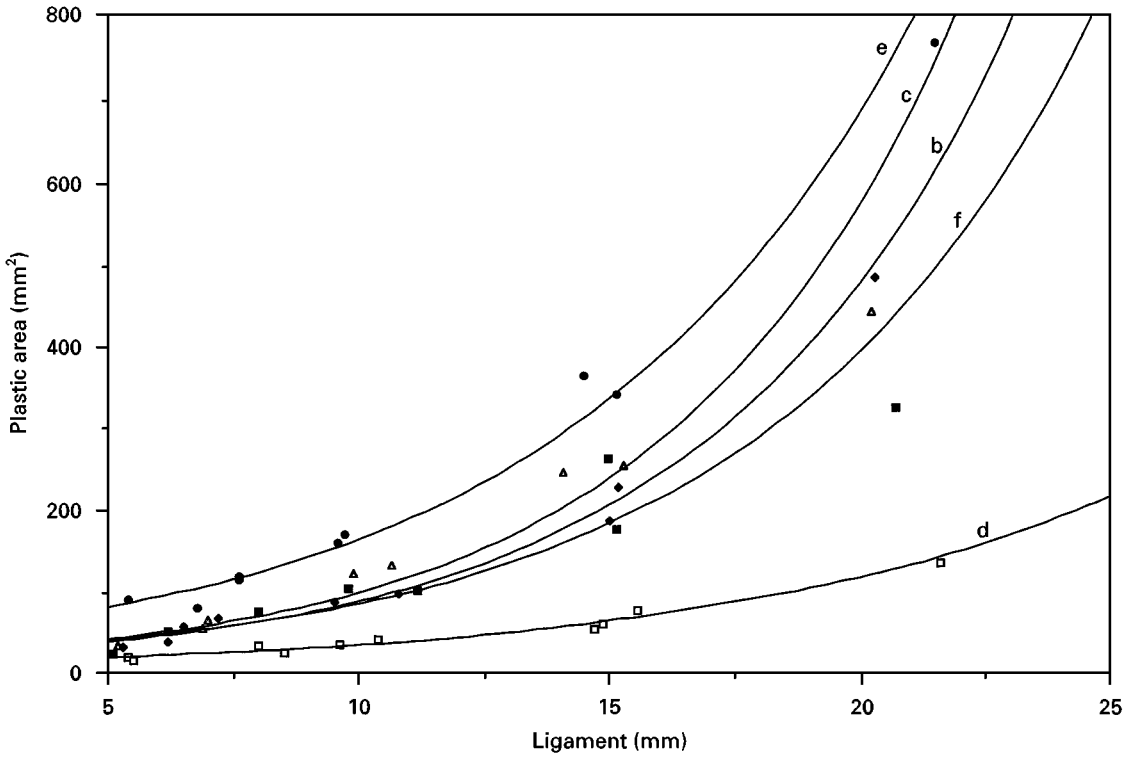

Figure 5 Plastic area calculated by adopting an elliptical shape as a function of ligament size for all hybrid composites. Symbols (associated with the solid curves labelled as in Fig. 2) indicate the experimental results.

with increasing amount of elastomer (see Table I) is probably related to the yielding behaviour of the composites.

3.3. Development of the plastic zone

LM pictures taken during fracture of DDENT specimens of 10 mm ligament are presented in Fig. 6. Fig. 6a shows a macroscopic brittle fracture of the pure PP specimen (featuring multiple crack bifurcations along the ligament). On a microscopic scale the fracture surface, i.e., process zone, of the pure PP showed ductile characteristics. Stable ductile crack growth is characteristic for all other composite specimens in which an elliptically shaped plastic zone (dark area) is formed. The plastic zone is given by "stress whitening" which is caused by density fluctuations due to crazing and voiding processes. The addition of 5 vol% SEBS to the base composite enhances the ductility and enlarges the plastic zone (see Fig. 6c). An even more pronounced ductilility can be stated for the blends with 20 vol% SEBS (see. Fig. 6e). Here dense

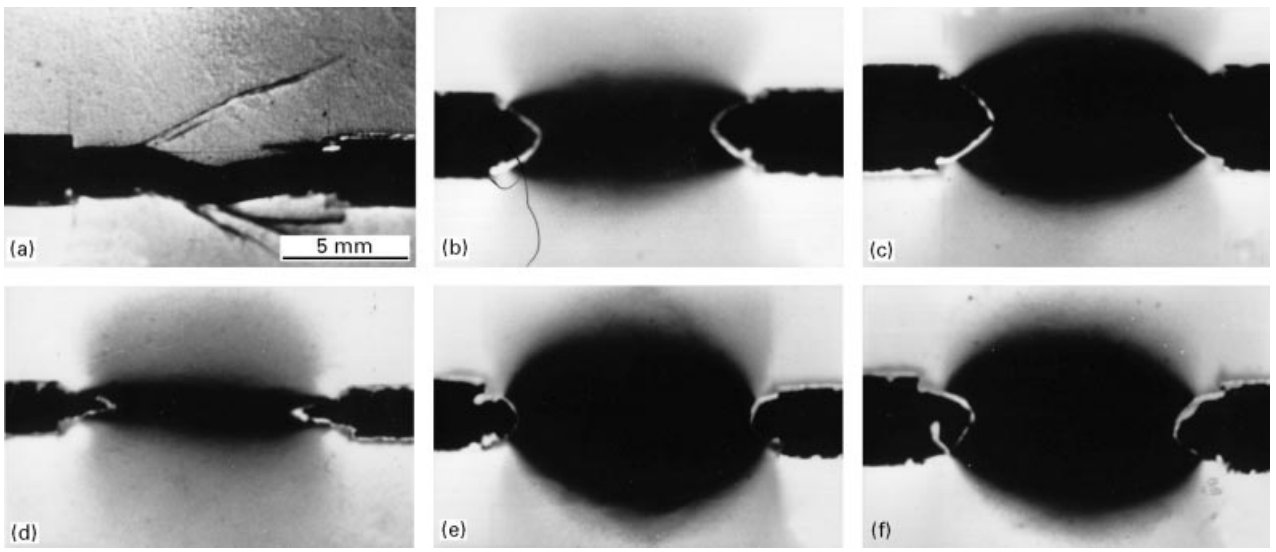

Figure 6 LM pictures taken during the loading of DDENT specimens at the same ligament length ($l = 10$ mm): (a) PP; (b) PP + 10 vol% GBs; (c) PP + 10 vol% GBs + 5 vol% SEBS; (d) PP + 10 vol% GBs + 5 vol% SEBS-g-MA; (e) PP + 10 vol% GBs + 20 vol% SEBS; (f) PP + 10 vol% GBs + 20 vol% SEBS-g-MA. Note that the stress-whitened plastic zone (turning dark in the LM pictures) is clearly visible.

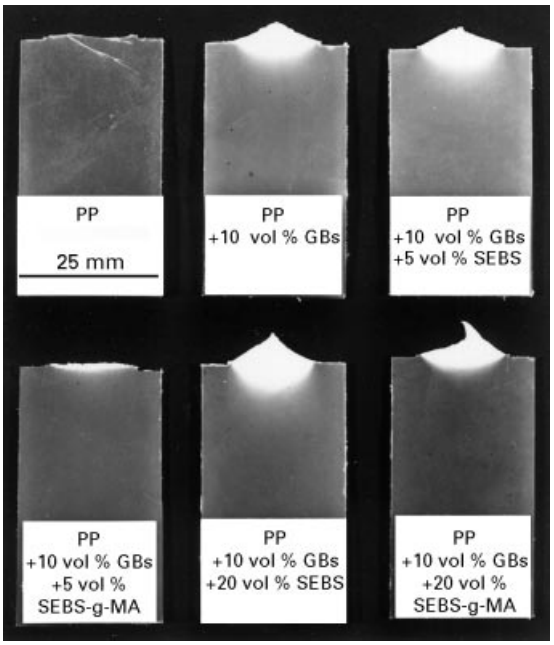

Figure 7 Macrophotographs taken from fractured DDENT specimens with a ligament of about 15 mm showing the stress-whitened plastic zone.

stress whitening and a maximum in the height of the plastic zone can be found. It should be mentioned here that stress-induced whitening was confirmed also for the bulk of the plastic zone (by sectioning it with a microtome), so that this is not just a surface phenomenon.

The incorporation of SEBS-g-MA resulted in restricted plastic deformations, well reflected in the reduction in the height of the plastic zone (see Fig. 6d and f and Fig. 7), especially when compared with the related composites containing SEBS (see Fig. 6c and e and Fig. 7). The macrophotographs taken from the fractured DDENT specimens (Fig. 7) corroborate the above statements.

IT frames taken during loading of a DDENT specimen of the base composite (PP + 10 vol% GBs) are presented in Fig. 8 together with the related σ–ε curve. The serial IT frames (the positions at which they were obtained are shown on the σ–ε curve) evidence the failure sequence. First, crack-tip blunting occurs followed by the onset of crack growth from both sides. More or less simultaneously to that the ligament starts to yield (see bright areas in Fig. 8A and B). This yielding is accompanied by an almost 2 °C rise in the local temperature field (see the corresponding cursor points in the view field). The IT pictures in Fig. 8B and C evidence the development of an elliptical plastic zone. Finally, the specimen fails by tearing as both cracks meet one another at the centre of the ligament (Fig. 8C). The temperature rise locally reaches 5 °C, as read from the Probeye scale in picture C.

Almost identical behaviour is observed for the base composite with 5 vol% SEBS elastomer. In Fig. 9A, as the stress reaches its maximum value, crack-tip blunting is evident. Just passing the maximum the ligament fully yields as can be deduced from pictures B and C in Fig. 9B and C. An interesting fact here is that

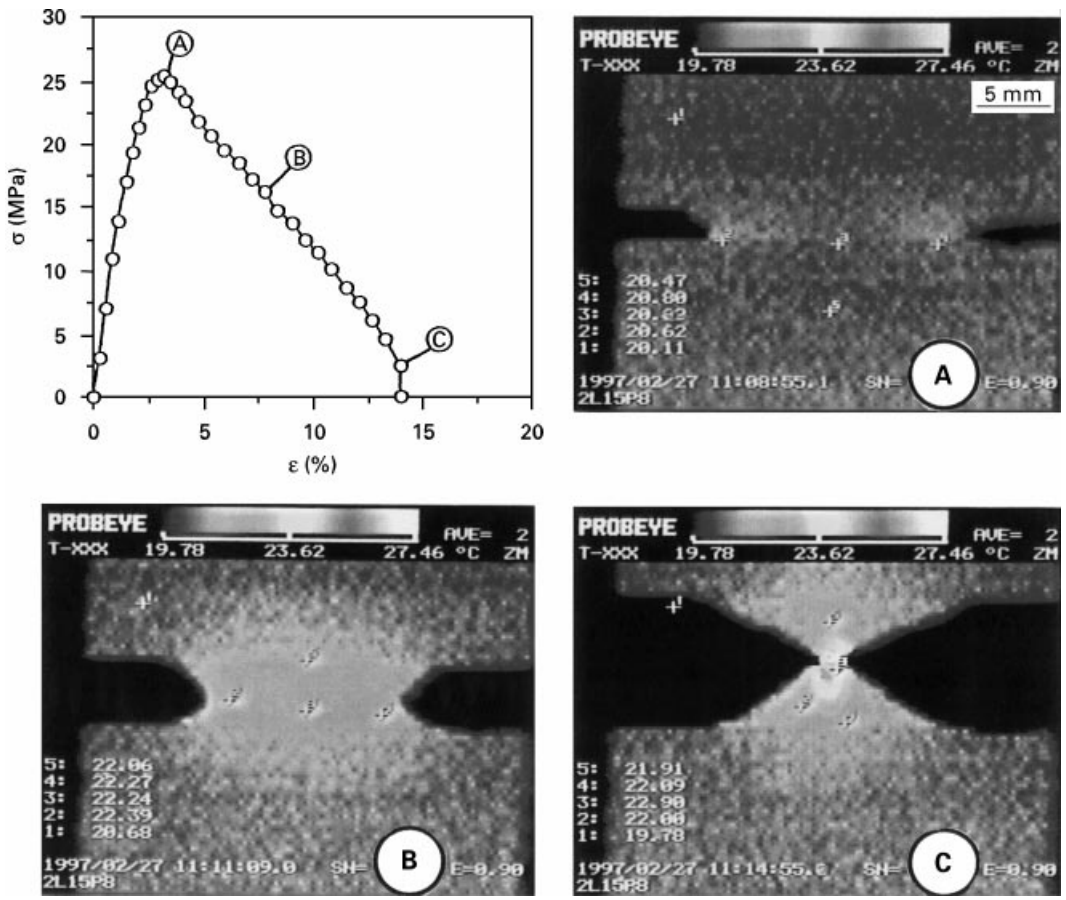

Figure 8 σ–ε curve together with serial IT pictures taken during loading of a DDENT specimen of the base composite (PP + 10 vol% GBs). Note that the recording points of the IT frames are indicated on the σ–ε curve.

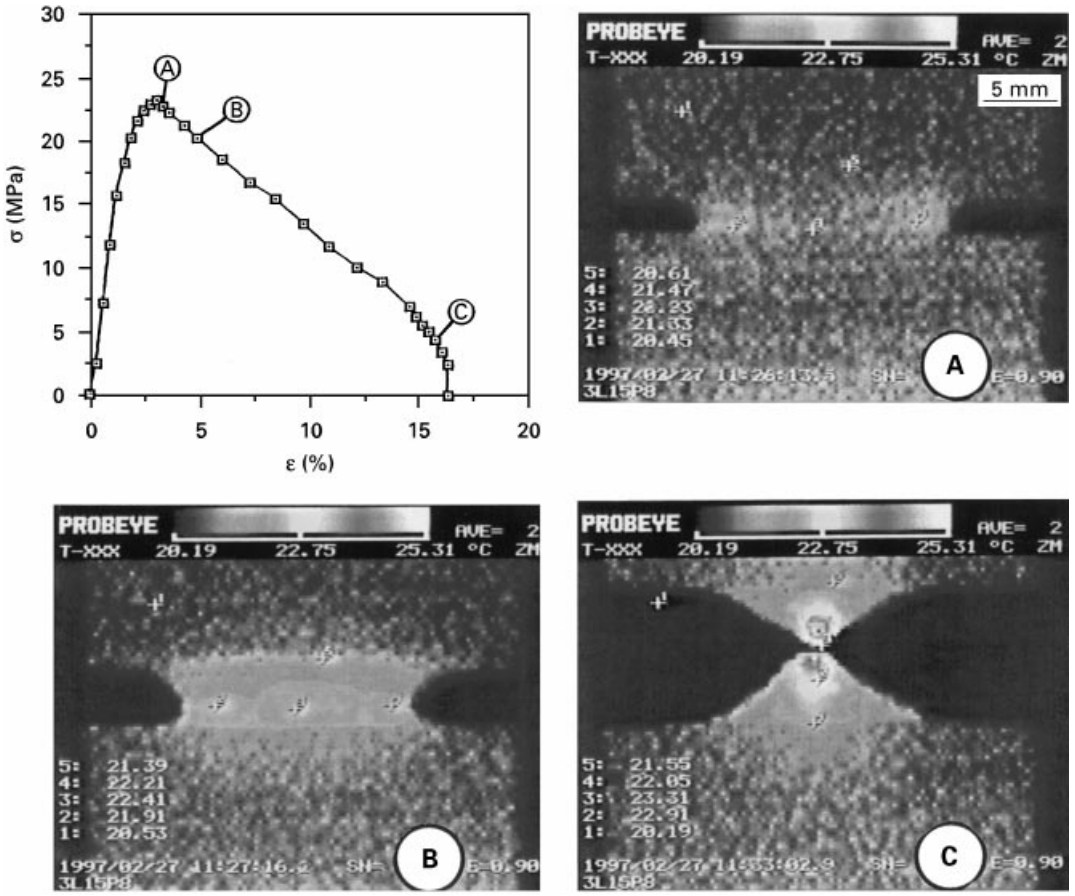

Figure 9 σ–ε curve together with serial IT pictures taken during loading of a DDENT specimen of the PP hybrid composite containing 10 vol% GBs + 5 vol% SEBS. For note see Fig. 8.

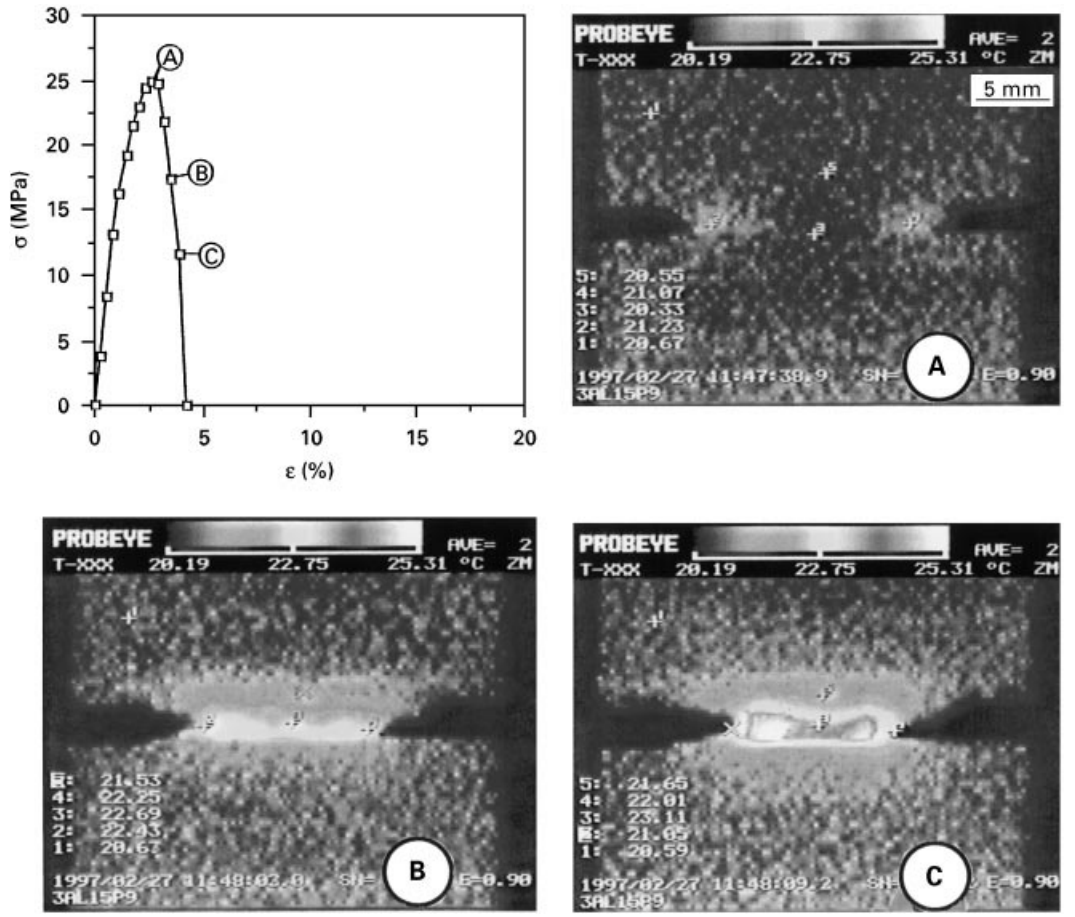

Figure 10 σ–ε curve together with serial IT pictures taken during loading of a DDENT specimen of the PP hybrid composite contaning 10 vol% GBs + 5 vol% SEBS-g-MA. For note see Fig. 8.

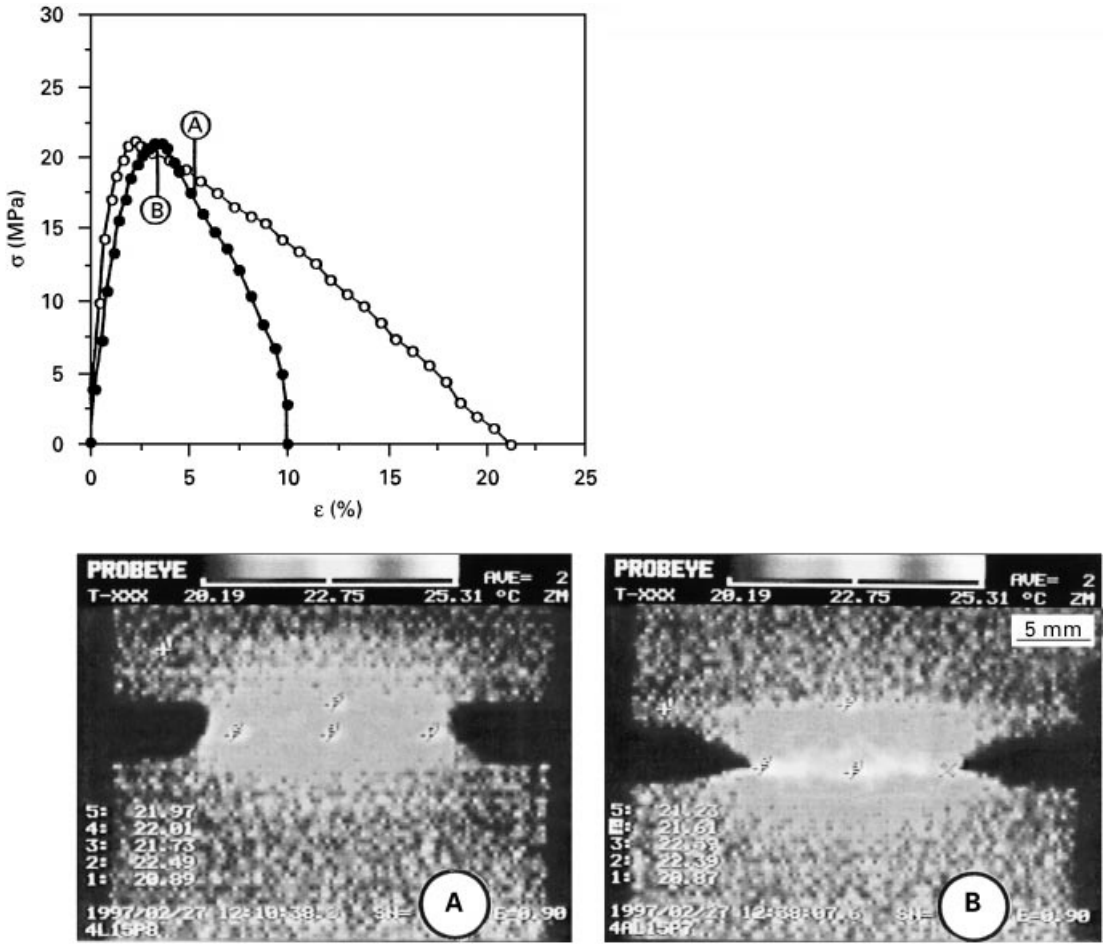

Figure 11 Comparison of the IT frames taken at comparable loading for the hybrid PP composites containg 10 vol% GBs and 20 vol% (A) SEBS and (B) SEBS-g-MA, respectively.

temperature rises locally (bright "hot spots" are visible) and not over all the ligament. This hints that the yielding is a time-dependent sequential process. It will be shown next that the failure process behind it relies on matrix cavitation followed by yielding (see next section). Again the plastic zone seems to adopt an elliptical shape (Fig. 9C). The final separation of the specimen is associated with a larger heat dissipation compared with the base composite (see Figs 8 and 9).

The fracture behaviour of the previous hybrid composite, however, with SEBS-g-MA elastomer is presented by the IT frames in Fig. 10. No clear crack-tip blunting (Fig. 10A) precedes the crack growth accompanied by a vigorous yielding of the ligament area (resulting in a high thermal emission rate; see bright area in Fig. 10B) are typical for this type of composite. Final fracture occurs quite shortly after yielding, where an unstable (fast) crack growth starts. Therefore, the related σ–ε curve experiences a sharp drop. The high thermal emission (the temperature is almost 5 °C higher at crack tips) indicates the presence of some local plane-strain field, which is not relieved as in case of the base and SEBS-containing composites. This failure mode agrees with the findings from LM, presented above (see Figs 6 and 7).

In order to demonstrate the exact influence of the MA grafting on the fracture response of the hybrids, two IT pictures were chosen from the failure sequence of the systems with 20 vol% elastomer without grafting (Fig. 11A) and with grafting (Fig. 11B) at the same ligament length. These frames represent similar loading conditions as seen by the experimental σ–ε curves involved in Fig. 11. It is clearly observable that the SEBS-containing composite exhibits a much larger plastic zone, but the actual temperature peaks are distinctly lower than those of the composite with SEBS-g-MA (see Fig. 11B). The IT pictures seem to support the suggestion (made with respect to w_p above, see Table I) of better adhesion between the composites' constituents. These findings are in good agreement with the related essential and plastic work data. Grafted SEBS containing hybrids are characterized by reduced w_e and β values, but with enhanced w_p data compared with the corresponding ungrafted specimens. This difference is obviously linked to changes in the energy absorption mechanisms in the hybrids when SEBS or SEBS-g-MA are present. A deeper understanding of this aspect was expected from the fractographic inspection of both process and plastic zones of the hybrid composites.

3.4. Fractography

SEM pictures reveal a ductile failure for the base composite (i.e., PP + 10 vol% GBs), as shown in Fig. 12a, where torn matrix fibrils dominate the fracture surface. Recall that, in the case of the plain PP, semiductile failure was resolved only in the process

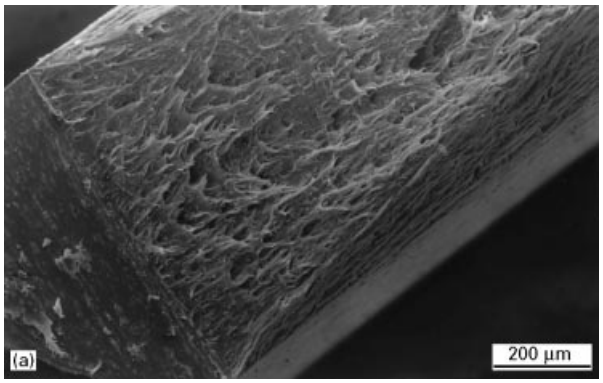

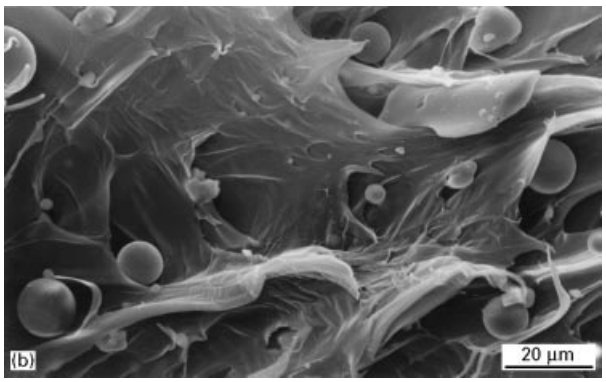

Figure 12 SEM pictures taken on the fracture surface (process zone) of a DDENT specimen of the base composite (PP + 10 vol% GBs).

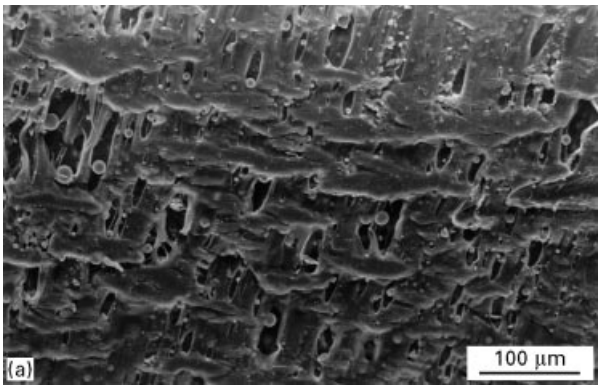

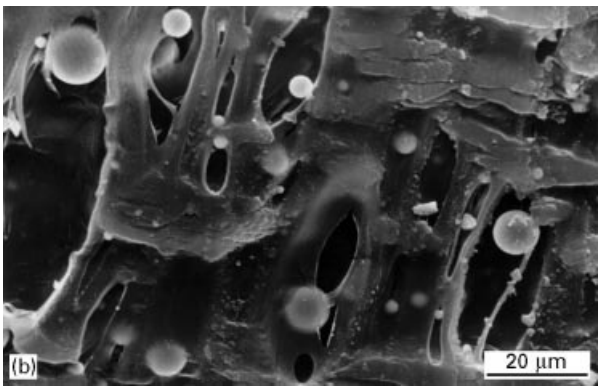

Figure 13 SEM pictures taken from the surface plastic zone of the DDENT specimen of the base composite. Note that the elliptical holes caused by cavitation together with their inclination to the loading direction are clearly visible. The loading direction was vertical.

zone (see Figs 6 and 7). The adhesion between PP and the GBs appears to be quite poor, especially on closer observation (Fig. 12b). Here crater-like formations in the PP matrix can be observed, in the centre of which GBs are nested.

The SEM pictures in Fig. 13 show the deformed ligament area (i.e., surface plastic zone) as photographed from the side of the same specimen presented in Fig. 12. GBs are located in elliptical ditches, which are oriented along the loading direction. The small offset between the direction of loading and crater's orientation is due to crack growth. The SEM pictures in Fig. 12 evidence that GBs induce matrix cavitation, i.e., voiding. This mechanism, termed also dewetting or debonding, is the first step in the failure sequence in composites with spherical fillers when the matrix modulus is lower than that of the filler (which is the usual case) [17]. Matrix shear bands accompanied by sparse crazing in the surface plastic zone are also easy to demonstrate (see Fig. 13a). Indeed, the toughening process of these hybrid composites appears to be quite complex but these mixed modes of fracture were previously observed for many particulate-reinforced polymers [9, 17, 18]. The voiding, supported by poor adhesion between particles and matrix, is supposed to relieve the local plane-strain stress field and thus can be made responsible for a change towards plane stress. The latter condition promotes shear yielding in PP. An analogous failure scenario was reported for filled toughened PP recently [19].

According to Wu [20] when the distance, τ, between two particles is above a critical value, an overlapping of the localized high stress fields occurs, enabling matrix shear yielding and further cavitating. This surface-to-surface critical distance, which is a function of the particle diameter, d, and volume fraction, V_f, can be expressed as [20]

$$\tau_c = d\left[\left(\frac{\pi}{6V_f}\right)^{1/3} - 1\right] \tag{4}$$

By substituting for $V_f = 0.1$ and $d = 10$ μm (maximum GB size) in Equation 4, $\tau_c = 7.5$ μm can be derived. For a GB mean size $d = 5$ μm this calculation yields $\tau_c = 4.0$ μm. Based on the SEM pictures in Fig. 13 both these distance requirements are satisfied and thus the prerequisite of a complex cavitation-yielding mechanism is confirmed.

Fracture surfaces of the composite consisting of PP + 10 vol% GB + 5 vol% SEBS are presented in Fig. 14. Again, a ductile mode of failure is predominant (multiple failed matrix fibrils protruding from the fracture surface are well resolved in Fig. 14). A closer examination of the fracture area at a higher magnification confirmed that a GB is not encapsulated by SEBS (which agrees with the findings of the former study [12]); the latter forms a separate disperse phase. The enhanced work-of-fracture parameters exhibited by these composites (see Fig. 3 and Table I) are related to the fracture mode. In the multiple-cavitation process, both GB and SEBS particles are involved. In addition to GBs, the SEBS particles also act as stress concentrators, causing the created stress fields to overlap and

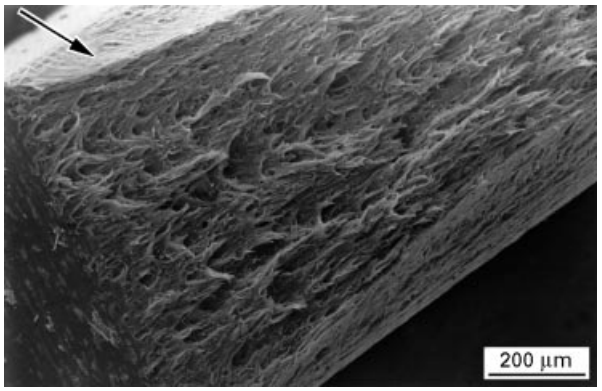

Figure 14 SEM pictures taken on the fracture surface of the hybrid composite consisting of PP + 10 vol% GBs + 5 vol% SEBS.

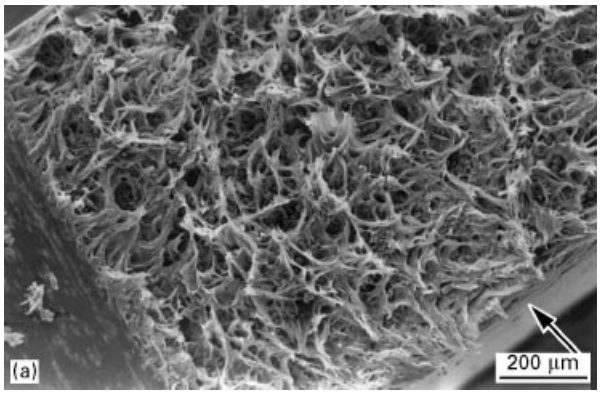

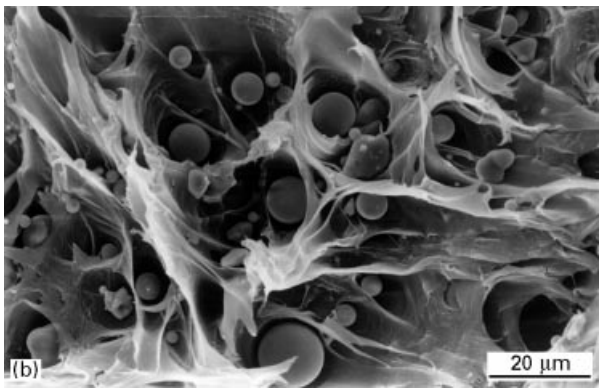

Figure 15 SEM picture taken on the fracture surface of the hybrid composite consisting of PP + 10 vol% GBs + 5 vol% SEBS-g-MA. The arrow indicates restricted necking (compare with Fig. 14).

triggering matrix yielding. As already discussed, the hybrid composites with SEBS-g-MA showed reduced toughness in comparison with the composites with SEBS elastomer. Fig. 15 refers to the specimens of the composite from PP + 10 vol% GBs + 5 vol% SEBS-g-MA. Although the fracture mode is ductile here as well (large cavities with concomitant matrix deformation are visible), the plastic zone is restricted. This agrees with the LM (see Figs 6 and 7) and IT results (see Fig. 10). In the SEM picture in Fig. 15b, the GB seems to be covered by the SEBS-g-MA elastomer (termed as core-shell formations in [12]). Because of this elastomer sheath the GBs tend to form aggregates (see Fig. 16a). This means that the average interparticle distance (by particles both GBs and elastomer are meant) is increasing and thus the conditions for yielding become less favourable. The adhesion between the PP matrix and the SEBS-g-MA coated GBs in these composites seems to be stronger (see Fig. 16a) than for the hybrid composites with SEBS. The rationale behind the reduced work of fracture data (see Table I) of the hybrids with GB and SEBS-g-MA is probably the following: since this elastomer tends to coat the GBs and thus results in a better adhesion between GBs and PP, the tendency to cavitation (debonding and dewetting) is substantially reduced. It is worth mentioning that the stress concentration scenario caused by particles in a polymer depends on the stiffness relation of particle and polymer (which is obviously changed by coating) [17]. Furthermore, the transition from plane strain toward plane stress is hampered locally owing to the lack of the finely dispersed elastomeric phase. Recall that the dispersed rubber particles, acting as "equatorial" stress concentrators, generate crazing [17], which is usually superimposed by multiple shear yielding in impact-modified PP [18, 19], including styrenic thermoplastic rubbers [21]. The shear yielding or shear flow process is, however, restricted since the SEBS-g-MA is present less in form of dispersed particles but mostly as a coating of the GBs. The plane-strain constraint is not relieved globally either, which leads to a premature failure in these hybrids. This is also confirmed by the restricted "necking' of the ligament area (arrow in Fig. 15a).

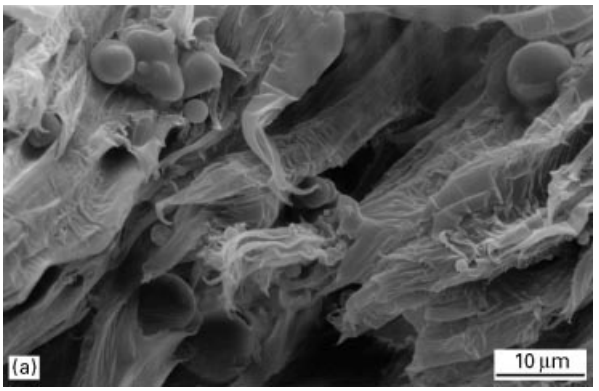

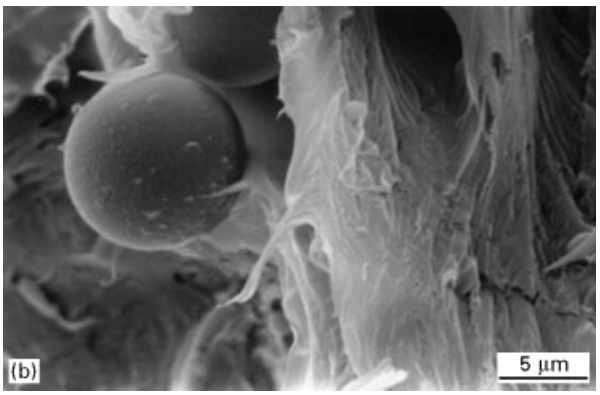

Figure 16 Higher-magnification SEM pictures on the fracture surface of the hybrid composite containing SEBS-g-MA.

The improved adhesion between the SEBS-g-MA coated GB and PP is responsible for the increase in w_p

compared with the hybrids with SEBS (see Table I). There is one more aspect to be clarified: why does w_p decrease with increasing elastomer content? (See Table I.) This can be attributed to a change in the yielding behaviour of the composites; yielding is strongly encouraged (i.e., both yield strength and strain are reduced, see also Fig. 2) by adding elastomer to PP.

4. Conclusions

Based on this study in which the EWF approach was adopted to make a toughness assessment of PP–GBs elastomer composites containing SEBS and SEBS-g-MA, respectively, the following conclusions can be drawn.

1. The incorporation of finely dispersed GBs did not affect the essential work parameter, w_e, but strongly influenced the non-essential or plastic work parameter, w_p of PP. Further addition of an elastomer to a base composite, composed of PP and 10 vol% GBs, affected both w_e and w_p. w_e increased with increasing elastomer content, whereas w_p seemed to go through a maximum as a function of the elastomer content. This feature proved to depend on the type of the elastomer, and thus on the microstructure of the hybrid composites.

2. The above trends in the toughness parameters were well reflected by the failure behaviour of the composites. GBs induced matrix cavitation, which triggered the yielding of the PP matrix, especially in the presence of a finely dispersed elastomer phase (i.e., SEBS, which acted as an other type of stress concentrator). Incorporation of SEBS-g-MA changed the morphology (this elastomer adhered to the GBs) and thus also the failure behaviour of the hybrids. Because of the good adhesion between the SEBS-g-MA coated GB and the PP, which is reflected in enhanced w_p values, the failure mode and sequence altered. This resulted in a pronounced size reduction of the plastic zone as confirmed by LM and IT.

Acknowledgement

The authors gratefully acknowledge the support of this work by the Deutsche Forschungsgemeinschaft (Ka 1202/3-1).

References

1. K. B. BROBERG, *Int. J. Fracture*, **4** (1968) 11.
2. *Idem. J. Mech. Phys. Solids* **23** (1975) 215.
3. J. WU and Y.-W. MAI, *Polym. Engng Sci*., **36** (1996) 2275.
4. J. KARGER-KOCSIS, *Polym. Bull.* **37** (1996) 119.
5. J. KARGER-KOCSIS, T. CZIGÁNY and E. J. MOSKALA, Polymer **38** (1997) 4587.
6. S. HASHEMI, *J. Mater. Sci.* **32** (1997) 1563.
7. E. MARTUSCELLI, in "Polypropylene: structure, blends and composites", Vol. 2, edited by J. Karger-Kocsis, (Chapman & Hall, London, 1995) ch. 4, pp. 95–140.
8. P. GALLI, J. C. HAYLOCK and T. SIMONAZZI, in "Polypropylene: structure, blends and composites", Vol. 2 edited by J. Karger-Kocsis (Chapman & Hall, London, 1995) ch. 1, pp. 1–24.
9. B. PUKÁNSZKY, in "Polypropylene: structure, blends and composites", Vol. 3 edited by J. Karger-Kocsis (Chapman & Hall, London, 1995) ch. 1, pp. 1–70.
10. V. A. MATONIS and N. C. SMALL, *Polym. Engng Sci*., **9** (1969) 90.
11. L. E. ASP, B. A. SJÖGREN and L. A. BERGLUND, *Polym. Compos.* **18** (1997) 9.
12. F. STRICKER and R. MÜLHAUPT, *J. Appl. Polym. Sci*., **62** (1996) 1799.
13. A. GRAY, "Testing protocol for essential work of fracture" (ESIS TC-4 Group, 1993).
14. J. KARGER-KOCSIS and T. CZIGÁNY, *Polym.* **37** (1996) 2433.
15. J. G. WILLIAMS, "Fracture mechanics of polymers" (Ellis Horwood, Chichester, West Sussex, 1987).
16. T. VU-KHANH, *Theor. Appl. Fract. Mech.* **21** (1994) 83.
17. L. E. NIELSEN and R. F. LANDEL, "Mechanical properties of polymers and composites" (Marcel Dekker, New York, 1994) p. 436.
18. G. H. MICHLER, Kunststoff-Mikromechanik (Hanser, München, 1992).
19. G.-M. KIM, G. H. MICHLER, M. GAHLEITNER and J. FIEBIG, *J. Appl. Polym. Sci.* **60** (1996) 1391.
20. S. WU, *ibid.* **35** (1988) 549.
21. J. KARGER-KOCSIS, L. KOLLÁR and Z. BALAJTHY, *Kunststoffe* **74** (1984) 104.

Received 12 June 1997
and accepted 5 February 1998